Characteristics of starch-based films with different amylose contents plasticised by 1-ethyl-3-methylimidazolium acetate

Fengwei Xie [a,*], Bernadine M. Flanagan [b], Ming Li [b], Rowan W. Truss [c], Peter J. Halley [a,c], Michael J. Gidley [b], Tony McNally [d], Julia L. Shamshina [e], Robin D. Rogers [e]

[a] *Australian Institute for Bioengineering and Nanotechnology, The University of Queensland, Brisbane, Qld 4072, Australia*

[b] *Centre for Nutrition and Food Sciences, Queensland Alliance for Agriculture and Food Innovation, The University of Queensland, Hartley Teakle Building, St Lucia, Qld 4072, Australia*

[c] *School of Chemical Engineering, The University of Queensland, Brisbane, Qld 4072, Australia*

[d] *International Institute for Nanocomposites Manufacturing (IINM), WMG, University of Warwick, CV4 7AL, UK*

[e] *Center for Green Manufacturing and Department of Chemistry, The University of Alabama, Tuscaloosa, AL 35487, USA*

[*] Corresponding author. Tel.: +61 7 3346 3199; fax: +61 7 3346 3973.

Email address: f.xie@uq.edu.au, fwhsieh@gmail.com (F. Xie).

ABSTRACT

Starch-based films plasticised by an ionic liquid, 1-ethyl-3-methylimidazolium acetate ([Emim][OAc]), were prepared by a simple compression moulding process, facilitated by the strong plasticisation effect of [Emim][OAc]. The effects of amylose content of starch (regular vs. high-amylose maize) and relative humidity (RH) during ageing of the samples on a range of structural and material characteristics were investigated. Surprisingly, plasticisation by [Emim][OAc] made the effect of amylose content insignificant, contrary to most previous studies when other plasticisers were used. In other words, [Emim][OAc] changed the underlying mechanism responsible for mechanical properties from the entanglement of starch macromolecules (mainly amylose), which has been reported as a main responsible factor previously. The crystallinity of the plasticised starch samples was low and thus was unlikely to have a major contribution to the material characteristics, although the amylose content impacted on the crystalline structure and the mobility of amorphous parts in the samples to some extent. Therefore, RH conditioning and thus the sample water content was the major factor influencing the mechanical properties, glass transition temperature, and electrical conductivity of the starch films. This suggests the potential application of ionic liquid–plasticised starch materials in areas where the control of properties by environmental RH is desired.

Keywords:

Starch; Ionic liquid; 1-Ethyl-3-methylimidazolium acetate; Plasticization; Amylose/amylopectin ratio; Relative Humidity; Electrical Conductivity

Chemical compounds studied in this article

Starch (PubChem CID: 24836924); Water (PubChem CID: 962); Glycerol (PubChem CID: 753); 1-Ethyl-3-methylimidazolium acetate (PubChem CID: 11658353)

1. Introduction

In recent years, great attention has been focused on polymers from renewable resources (biopolymers: cellulose, starch, chitosan, chitin, etc.; bio-based polymers: poly(lactic acid) (PLA), polyhydroxyalkanoates (PHA), etc.) due to their availability, renewability, biocompatibility, and biodegradability (Yu, Dean, & Li, 2006). Among these groups of polymers, starch grows in plants and is naturally structured in a hierarchical multi-level complex form: from macro-observation, starch is in the form of granules (<1 μm~100 μm); many granules are broadly composed of alternating amorphous and semicrystalline shells (growth rings) (100~400 nm); the semicrystalline shell is stacked crystalline and amorphous lamellae (periodicity) (9~10 nm); with all structures based on two major biomacromolecules called amylose (mainly linear) and amylopectin (hyper-branched) (~nm) (Fu, Wang, Li, Wei, & Adhikari, 2011; Jane, 2009; Pérez, Baldwin, & Gallant, 2009; Pérez & Bertoft, 2010). For the utilisation of starch, it is important to understand this complex structure and how it can be altered to achieve desired forms (e.g. a plasticised form).

With a plasticiser and elevated temperature, a process known as “gelatinisation” (with abundant plasticiser content) or “melting” (with limited plasticiser content) occurs, resulting in disruption of the 3D structure of native starch; and, if preferential conditions

63 are reached, this can result in a homogeneous amorphous material known as
64 “thermoplastic starch” or “plasticised starch”, which is essential in the production of
65 some starch-based materials (Avérous, 2004; Liu, Xie, Yu, Chen, & Li, 2009a; Xie,
66 Halley, & Avérous, 2012; Xie, Pollet, Halley, & Avérous, 2013). While water is the
67 most commonly used plasticiser for starch, substances such as polyols (glycerol, glycol,
68 sorbitol, etc.), compounds containing nitrogen (urea, ammonium derived, amines), and
69 citric acid have also been reported to be effective in the plasticisation of starch (Liu et al.,
70 2009a; Xie et al., 2012). A plasticiser for starch should preferably be stable (non-volatile)
71 both during thermal processing and in post-processing stages, be ineffective in starch
72 macromolecular degradation, be safe to humans and the environment, and be able to
73 provide starch-based materials with enhanced performance and new capabilities.
74 Unfortunately, the currently-used plasticisers do not yet have all the desired attributes and
75 thus finding alternative and better plasticisers for starch is of interest.
76 Ionic liquids, often referred to as “green solvents”, have the capability of dissolving
77 many substances, including many organic polymers, and have good properties such as
78 chemical and thermal stability, low vapour pressure, and high ionic activity (Lu, Yan, &
79 Texter, 2009). Many ILs, especially ones based on the imidazolium cation, have been
80 shown to be capable of dissolving polysaccharides such as starch (Biswas, Shogren,
81 Stevenson, Willett, & Bhowmik, 2006; El Seoud, Koschella, Fidale, Dorn, & Heinze,
82 2007; Wilpiszewska & Spychaj, 2011; Zakrzewska, Bogel-Łukasik, & Bogel-Łukasik,
83 2010; Zhu et al., 2006), cellulose (Heinze, Schwikal, & Barthel, 2005; Zhang, Wu, Zhang,
84 & He, 2005), chitin/chitosan (Wu, Sasaki, Irie, & Sakurai, 2008; Xie, Zhang, & Li, 2006),
85 silk fibroin (Phillips et al., 2004; Wang, Chen, Yang, & Shao, 2012; Wang, Yang, Chen,

& Shao, 2012), lignin (Pu, Jiang, & Ragauskas, 2007), zein protein (Biswas et al., 2006), wool keratin (Xie, Li, & Zhang, 2005); and thus can be used as excellent media for polysaccharide plasticisation and modification. Moreover, the use of ILs may also allow for the development of starch-based ionically conducting polymers or solid polymer electrolytes (Liew, Ramesh, Ramesh, & Arof, 2012; Ramesh, Liew, & Arof, 2011; Ramesh, Shanti, Morris, & Durairaj, 2011; Ramesh, Shanti, & Morris, 2012; Wang, Zhang, Liu, & He, 2009a; Wang, Zhang, Wang, & Liu, 2009b; Wang, Zhang, Liu, & Han, 2010b). Nevertheless, work reported to date mostly involved processing in solution, whereas melt processing should be more relevant to industry application as much less solvent is required and higher efficiency is expected. Sankri et al. (2010) and Leroy, Jacquet, Coativy, Reguerre, and Lourdin (2012) have done pioneering work using an IL (1-butyl-3-methylimidazolium chloride, or [Bmim][Cl]) as a new plasticiser for melt processing of starch-based materials, which demonstrated improved plasticisation, electrical conductivity, and hydrophobicity. Our previous work (Xie et al., 2014) has shown that an IL, 1-ethyl-3-methylimidazolium acetate ([Emim][OAc]), has a significant plasticisation effect including for a high-amylose starch, prepared via a simple compression moulding process; and can reduce the crystallinity and make the amorphous phase more mobile, advantageous for some specific applications (e.g. electrically conductive materials).

This paper reports studies aimed at understanding the plasticisation effect of starch by ILs. Based on the established protocol (Xie et al., 2014), we investigate how the amylose content of starch can influence the characteristics of starch-based materials plasticised by the IL, [Emim][OAc]. It is well established that the amylose content can greatly

influence starch granule architecture and molecular structure (Blazek et al., 2009; Cheetham & Tao, 1997; Jenkins & Donald, 1995; Shi, Capitani, Trzasko, & Jeffcoat, 1998), thermal behaviour (Liu, Yu, Xie, & Chen, 2006; Liu et al., 2011), processing and rheological behaviour (Chaudhary, Miler, Torley, Sopade, & Halley, 2008; Chinnaswamy & Hanna, 1988; Della Valle, Colonna, Patria, & Vergnes, 1996; Li et al., 2011; Wang et al., 2010a; Xie et al., 2009), and the structure and properties of resulting starch-based materials (Chaudhary, Torley, Halley, McCaffery, & Chaudhary, 2009; Cheetham & Tao, 1998; Forssell, Lahtinen, Lahelin, & Myllärinen, 2002; Li et al., 2011; Lourdin, Della Valle, & Colonna, 1995; Mondragón, Mancilla, & Rodríguez-González, 2008; Rindlav-Westling, Stading, & Gatenholm, 2001; Rindlav-Westling, Stading, Hermansson, & Gatenholm, 1998; van Soest & Borger, 1997). In order to reveal the effect of amylose content in the current study, a simple one-step compression moulding process was employed to minimise the effect of shear-induced macromolecular degradation during processing. Moreover, considering that starch is a hydrophilic biopolymer sensitive to environmental moisture and that [Emim][OAc], an hydrophilic IL, may have some impact on the hydrophilicity of starch-based materials, the effect of relative humidity (RH) during ageing of the materials on the material characteristics was also investigated. Thus, the plasticisation effects of [Emim][OAc] on the crystalline structure, mechanical properties, glass transition temperature, thermal stability, and electrical conductivity of the starch-based films are reported here, with the aim of providing information for designing starch plasticisation processes and starch-based materials with tailored properties.

2. Materials and Methods

2.1. Materials

Two commercially available maize starches, Gelose 80 (G80) and regular maize starch (RMS) were used in this work. RMS was supplied by New Zealand Starch Ltd. (Onehunga, Auckland, New Zealand) with the product name Avon Maize Starch; and G80 was supplied by Ingredion ANZ Pty Ltd (Lane Cove, NSW, Australia). Both starches were chemically unmodified and their amylose contents were 24.4% and 82.9%, respectively, as measured previously (Tan, Flanagan, Halley, Whittaker, & Gidley, 2007). The original moisture content of the two starches were 14.1 wt.% and 14.4 wt.% respectively, as measured by a Satorius Moisture Analyser (Model MA30, Sartorius Weighing Technology GmbH, Weender Landstraβe 94–108, 37075, Goettingen, Germany). Deionised water was used in all instances. Glycerol (AR) was supplied by Chem-Supply Pty Ltd (Gillman, SA, Australia) and used as received. [Emim][OAc] of purity ≥95%, produced by IoLiTec Ionic Liquids Technologies GmbH (Salzstraβe 184, D-74076 Heilbronn, Germany), was also supplied by Chem-Supply Pty Ltd. [Emim][OAc] was used as received without further purification. As [Emim][OAc] was liquid at room temperature miscible with water (Mateyawa et al., 2013), different ratios of water–[Emim][OAc] mixture could be easily prepared in vials for subsequent use.

2.2. Sample preparation

Formulations for sample preparation are shown in Table 1. In Table 1 and the following text, the plasticised starch samples are coded in the format of "G80-18-L", where "G80" denotes the type of starch, "18" indicates the weight content of the ionic

liquid, and "L" means the RH during conditioning (either L, low, 33%; M, medium, 52%; or H, high, 75%). Based on our preliminary work (Xie et al., 2014), the added water–[Emim][OAc] mixture content was fixed at 30% by weight on the basis of the starch wet weight. The liquid mixture was added drop-wise to the starch, accompanied by careful blending using a mortar and pestle to ensure an even distribution of the liquid mixture in the starch. Then, the blended samples were hermetically stored in ziplock bags at 4 °C for at least overnight, before thermal compression moulding. This allowed time for further equilibration of the samples. The powder was carefully and equally spread over the moulding area with poly(tetrafluoroethylene) glass fabrics (Dotmar EPP Pty Ltd, Acacia Ridge, Qld, Australia) located between the starch and the mould, then compression moulded at 160 °C and 6 MPa for 10 min, followed by rapidly cooling to room temperature (RT) before opening the mould and retrieving the sample (thickness approx. 1.2 mm). The films were conditioned at different RHs, 33% (over saturated magnesium chloride solution), 52% (over saturated magnesium nitrate solution), and 75% (over saturated sodium chloride solution), at RT in desiccators for one month before any characterisation of the materials. After the conditioning, the thickness of the films was about 1 mm. The final water contents in the conditioned samples were calculated based on the weight data before and after vacuum-oven drying at 100 °C for two days.

[Insert Table 1 here]

According to our preliminary work (Xie et al., 2014), the use of compression moulding under the described conditions should mostly destroy the starch granules so that plasticised starch could be formed.

2.3. Characterisation

2.3.1. X-ray diffraction (XRD)

The starch samples were placed in the sample holder of a powder X-ray diffractometer (D8 Advance, Bruker AXS Inc., Madison, WI, USA) equipped with a graphite monochromator, a copper target, and a scintillation counter detector. XRD patterns were recorded for an angular range (2θ) of 4–40°, with a step size of 0.02° and a step rate of 0.5 s per step, and thus the scan time lasted for approximately 15 min. The radiation parameters were set as 40 kV and 30 mA, with a slit of 2 mm. Traces were processed using the Diffracplus Evaluation Package (Version 11.0, Bruker AXS Inc., Madison, WI, USA) to determine the X-ray diffractograms of the samples. The degree of crystallinity was calculated using the method of Lopez-Rubio, Flanagan, Gilbert, and Gidley (2008) with the PeakFit software (Version 4.12, Systat Software, Inc., San Jose, CA, USA), Eq. (1):

$$X_c = \frac{\sum_{i=1}^{n} A_{ci}}{A_t} \qquad (1)$$

where A_{ci} is the area under each crystalline peak with index i, and A_t is the total area (both amorphous background and crystalline peaks) under the diffractogram.

The V-type crystallinity (single-helical amylose structure) was calculated based on the total crystalline peak areas at 7.5, 13, 20, and 23° (van Soest, Hulleman, de Wit, & Vliegenthart, 1996).

2.3.2. NMR

The rigid components (short-range orders and rigid amorphous starch) of the starch-based films were examined by solid-state ^{13}C cross-polarization magic angle spinning nuclear magnetic resonance (^{13}C CP/MAS NMR) experiments at a ^{13}C frequency of 75.46 MHz on a Bruker MSL-300 spectrometer. Using scissors, the sheets were cut into small evenly sized pieces and were packed in a 4-mm diameter, cylindrical, PSZ (partially-stabilized zirconium oxide) rotor with a KelF end cap. The rotor was spun at 5 kHz at the magic angle (54.7°). The 90° pulse width was 5 μs and a contact time of 1 ms was used for all samples with a recycle delay of 3 s. The spectral width was 38 kHz, acquisition time 50 ms, time domain points 2 k, transform size 4 k, and line broadening 50 Hz. At least 2400 scans were accumulated for each spectrum. Spectra were referenced to external adamantane and analysed by resolving the spectra into ordered and amorphous sub-spectra and calculating the relative areas as described previously (Tan et al., 2007).

The amounts of "mobile amorphous starch" and "rigid amorphous starch" were calculated according to our method reported previously (Xie et al., 2014). Briefly, it was assumed that all the crystalline starch was described by the XRD crystal-defect fitting. Then, the difference in the percentage between amorphous starch calculated from XRD

and that from ^{13}C CP/MAS NMR was considered to be due to the mobile amorphous starch.

2.3.3. Tensile testing

Tensile tests were performed with an Instron® 5543 universal testing machine (Instron Pty Ltd, Bayswater, Vic., Australia) with a 500 N load cell on dumbbell-shaped specimens cut from the sheets with a constant deformation rate of 10 mm/min at room temperature. The specimens corresponded to Type 4 of the Australian Standard AS 1683:11 (ISO 37:1994), and the testing section of each specimen was 12 mm in length and 2 mm in width. Young's modulus (E), tensile strength (σ_t), and elongation at break (ε_b) were determined by the Instron® computer software, from at least 7 specimens for each of the plasticised starch samples.

2.3.4. Dynamic mechanical thermal analysis (DMTA)

Dynamic mechanical thermal analysis (DMTA) was performed on rectangular sections taken from tensile bars of the plasticised starch samples using a Rheometric Scientific™ DMTA IV machine (Rheometric Scientific, Inc., Piscataway, NJ, USA) in the dual cantilever bending mode from −100 to 110 °C, with a heating rate of 3 K/min, a frequency of 1 Hz, and a strain value of 0.05%. The dynamic storage modulus (E'), loss modulus (E''), and loss tangent ($\tan \delta = E''/E'$) were obtained. To prevent water evaporation during the measurements, the specimens were coated with Vaseline grease. No swelling of the specimens was observed, suggesting no adverse effect of the Vaseline.

2.3.5. Thermogravimetric analysis (TGA)

A Mettler Toledo TGA/DSC1 machine (Mettler-Toledo Ltd., Port Melbourne, Vic., Australia) was used with 40 μL aluminium crucibles for thermogravimetric analysis (TGA) under nitrogen. A sample mass of about 5 mg was used for each run. The samples were heated from 25 °C to 550 °C at 3 K/min.

2.3.6. Electrical conductivity

Volume resistivity measurements were performed on the different starch-based films. The resistivity of samples (circular with diameter of 60 mm) was measured in triplicate using a Keithley electrometer (Model 6517A, Keithley Instruments, Inc., Cleveland, OH, USA) equipped with an 8009 test fixture and employing the Keithley Alt-Polarity method. The sample of interest was placed between two annular electrodes and the volume resistivity measured by applying a DC voltage potential across opposite sides of the sample and measuring the resultant current through the sample. This test conforms to ASTM D-257. The corresponding electrical conductivity values were obtained as the inverse of the volume resistivity values.

3. Results and Discussion

3.1. Moisture contents

While different formulations were used for preparing the samples, the water contents in the final samples could be largely varied by compression moulding and conditioning. Table 1 shows that the final water content was both affected by the original IL content and the RH during conditioning, but not the starch type — generally for both starches a

higher IL content and/or a higher RH during conditioning could lead to a higher final water content. It is noteworthy that except G80-27-H and RMS-27-H, the final water contents were lower than the water contents in original formulations, meaning that water desorption occurred during conditioning for most of the samples. This could suggest that there were very strong interactions between the IL and the starch, so both of them had much smaller chance to interact with water. In this case, the free water could mostly evaporate to the environment during the long-time conditioning. Unlike previous studies of solutions of starch, water and [Emim][OAc] (Mateyawa et al., 2013) where preferential interactions between water and the IL were proposed, the current work involves formulations containing starch as the main component for melt processing. Thus, although the water–[Emim][OAc] mixture was initially added into the starch (and strong interactions between [OAc^-] anions and water could firstly form (Hall et al., 2012)), during conditioning the IL might change to preferably interact with the abundant starch hydroxyls, resulting in its dissociation with water. Previous studies have suggested that IL anions could act as proton acceptors to form hydrogen bonding with the biopolymer hydroxyls (Abe, Fukaya, & Ohno, 2012; Fukaya, Sugimoto, & Ohno, 2006; Remsing, Swatloski, Rogers, & Moyna, 2006; Zhang et al., 2014). Nonetheless, the mechanism for the change of interactions shown in the current work is worth further investigation.

3.2. Structural characteristics

Figure 1 shows the XRD patterns of the two native starches and their plasticised samples. Native G80 showed a strong diffraction peak at a 2θ position of around 17°,

with a few smaller peaks at 2θ of approximately 5°, 10°, 14°, 15°, 19°, 22°, 23°, 26°, 31°, and 34°, indicative of B-type crystalline structure (Cheetham & Tao, 1998; Tan et al., 2007). After processing, besides the original B-type characteristic peaks (main peak at 2$\theta \approx 17°$), all the starch samples displayed peaks at 2θ of around 7°, 13°, 20°, and 22°, characteristic of V_H-type crystalline structure, a single-helical amylose structure (similar to that formed by amylose–lipid helical complexes) and is well known for thermally-processed (e.g., compression moulding and extrusion) starch-based materials (van Soest et al., 1996). That is, the plasticised samples contained crystalline structure not destructured by compression moulding (which is normal in starch processing) and some newly formed V_H-type crystalline structure mainly induced by processing (and possibly also some newly formed B-type crystalline structure during ageing with moisture) (van Soest et al., 1996; van Soest & Borger, 1997).

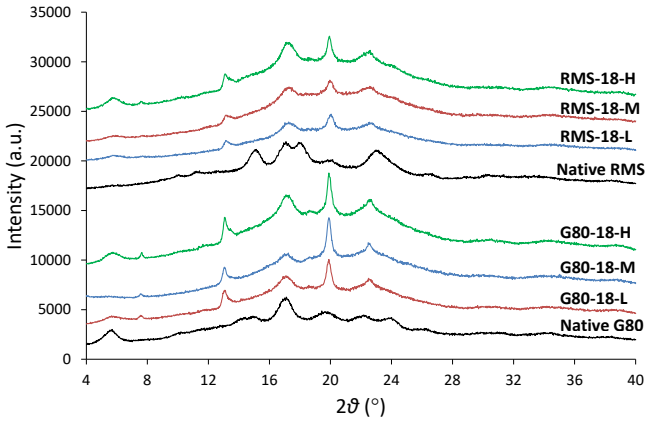

Figure 1 XRD results of G80 and RMS native starches and the different starch-based films. "L", "M", and "H" (shown by different colours) correspond to samples after conditioning at low (33%), medium (52%) and high (75%) relative humidity.

On the other hand, it can be seen from Figure 1 that native RMS showed typical A-type pattern, with strong reflections at 2θ of about 15° and 23° and an unresolved doublet at 2θ of 17° and 18°, with a few weak peaks at 2θ of about 26°, 30°, and 33° (Cheetham & Tao, 1998; Tan et al., 2007). For the plasticised samples, the doublet at 2θ of 17° and 18° disappeared, suggesting a complete loss of A-type pattern. Besides, the plasticised samples displayed strong V_H-type pattern as shown by sharp peaks at 2θ of 7°, 13°, 20°, and 22° (van Soest et al., 1996), and B-type pattern as indicated by strong reflections at 2θ of 5° and 17° (Cheetham & Tao, 1998; Tan et al., 2007). As for the plasticised G80 samples, the plasticised RMS has both (newly formed) V_H-type and B-type crystalline structures.

Table 2 shows the contents of double-helices (A- or B-type crystalline structure), single-helices (V-type crystalline structure), and amorphous parts of the plasticised starch samples as measured by XRD and NMR. Native G80 has a degree of crystallinity of 32.2%, and this value was greatly reduced in the processed and plasticised samples. Native RMS has a higher degree of crystallinity, 39.5%, which also decreased significantly after processing. The plasticised G80 samples overall had a higher degree of total crystallinity compared with the RMS samples. This could be because of the higher amount of double-helices remaining (and/or formed during processing), and the higher content of V-type crystalline structure formed in the plasticised G80 samples. However, for both starches no apparent difference in total crystallinity could be seen as a result of the different conditioning RHs, although the diffraction peaks were sharper after

higher RH conditioning, showing that crystallites within the sample were either larger or more perfect. It could be possible that the IL, which was more effective in the interaction with starch, governed the disruption of original crystalline structure as well as the formation of new crystalline structure, making the effect of environmental RH, and thus the sample water content, much less important. Moreover, it can be seen from Table 2 that the G80-based films had a higher mobile amorphous component (%) than that of the RMS films. As the sample water content was not apparently affected by the starch type, the differences in mobile amorphous component could be associated with the higher amylose content in G80. When plasticised by the IL, the linear amylose molecules could be more mobile than the highly short-branched amylopectin molecules. The more rigid molecular structure of amylopectin has already been proposed elsewhere (Liu, Halley, & Gilbert, 2010; Xie et al., 2009).

[Insert Table 2 here]

3.3. Mechanical properties

Figure 2 shows the tensile mechanical properties of the different starch samples. A higher content of [Emim][OAc] contributed to lower σ_t and E, as reported previously (Xie et al., 2014). In addition, σ_t and E also decreased as the RH (and thus the sample water content) increased. Since XRD and NMR results have already shown the insignificance of RH on starch molecular and crystalline orders and that crystallinity was

mostly low, the trend observed here is most likely due to the plasticisation effect of [Emim][OAc] and water (although [Emim][OAc] might be more important based on the discussion on moisture contents). Both the IL and water could disrupt hydrogen bonding between starch molecules, and form hydrogen bonding with the –OH sites of starch, resulting in reduced strength and stiffness. Additionally, there was little apparent effect of amylose content on σ_t or E (noting that with certain formulations and conditioning RHs, the final water contents were quite similar in different amylose-content samples) except that G80-9 had higher σ_t values than those of RMS-9. It is proposed that when the material is well plasticised, the macromolecular structure (amylose or amylopectin) plays a minor role in determining mechanical properties. That is, the entanglement of macromolecules (mainly amylose) is not a major influence on mechanical properties.

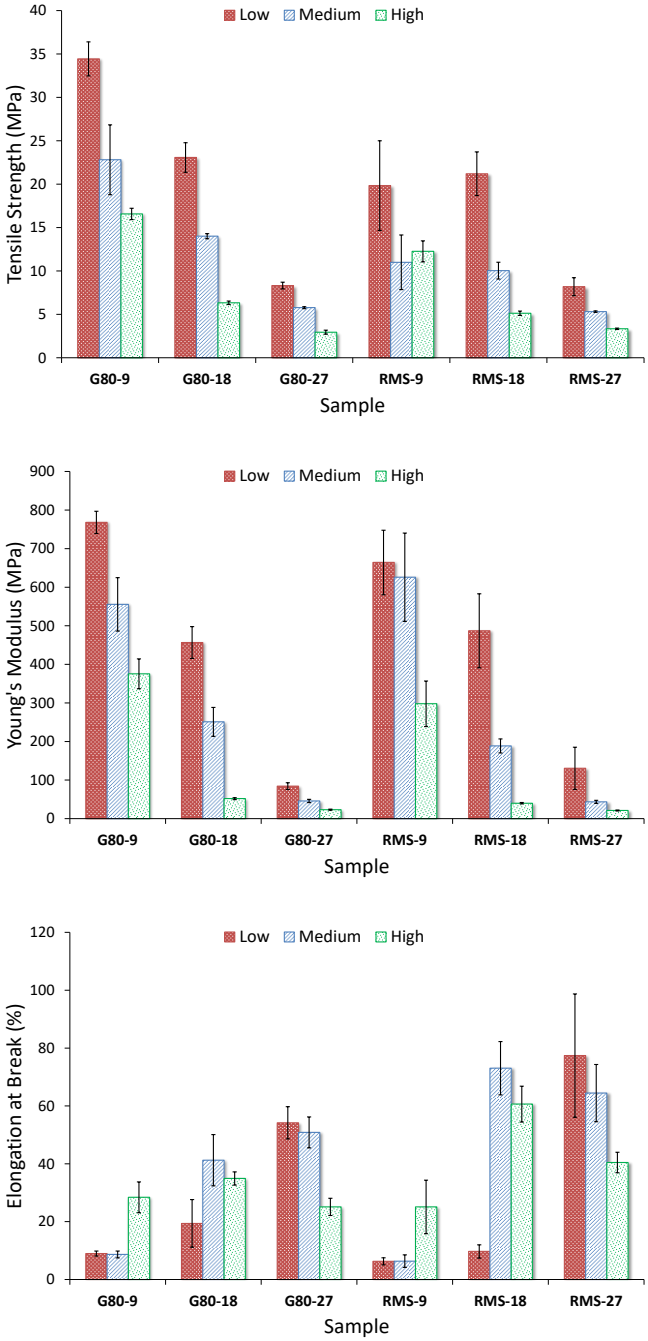

Figure 2 Tensile strength (σ_t) (upper), Young's modulus (E) (middle), and elongation at break (ε_b) (lower) of the different starch-based films. The error bars represent standard deviations. "Low", "Medium", and "High" (shown by different colours and patterns) correspond to samples after conditioning at low (33%), medium (52%) and high (75%) relative humidity.

The ε_b value was also affected by the RH (and thus the sample water content), but in a more complex way. It was observed from Figure 2 that increase in RH could either increase or decrease ε_b, depending on [Emim][OAc] content. When the [Emim][OAc] content was 18 wt.%, increase in RH initially increased ε_b remarkably and then decreased this value to some extent. Nevertheless, when the [Emim][OAc] content was 27%, increase in RH from 33% to 75% decreased ε_b progressively. It is proposed that the IL could disrupt starch H-bonding and prevent macromolecular entanglement, making the polymer have less "connections" between its chains and become "weaker". And also when the material was "softened" too much by plasticisation, there was no work hardening to stabilise drawing, as indicated by increased ε_b. In addition, it can be noticed that when the material was well plasticised but not "too soft" (the [Emim][OAc] content 18%), RMS could lead to a higher value of ε_b than that for G80. This differs from the results of extruded starch-based films that show higher ε_b in starch with a higher amylose content (Li et al., 2011). Here with, again, much less entanglement of macromolecules (mainly amylose) due to the plasticisation by [Emim][OAc], the major reason accounting for the moderately higher ε_b for the RMS samples might be the much bigger size of amylopectin macromolecules which could be stretched more before breaking.

3.4. DMTA analysis

Figure 3 shows the DMTA results of the different starch samples. For some of the samples, a prominent peak was shown between 30 °C and 100 °C. Based on previous

studies (Madrigal, Sandoval, & Müller, 2011; Perdomo et al., 2009), this peak can be attributed to the glass transition of starch (T_g), which will be the main focus of the discussion below. Prior to this peak, another moderate peak can be seen at a lower temperature (between –80 °C and 30 °C depending on sample) which can be ascribed to the glass transition of plasticiser-rich domains.

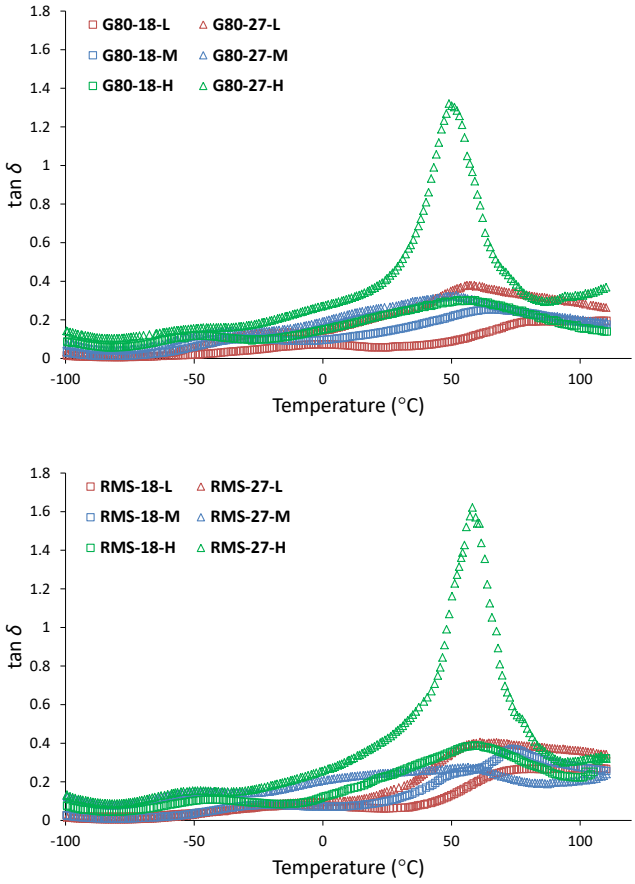

Figure 3 tan δ of the different starch-based films (top: G80; bottom: RMS). "L", "M", and "H" (shown by different colours) correspond to samples after conditioning at low (33%), medium (52%) and high (75%) relative humidity.

It can be seen from Figure 3 that, for both G80 and RMS, the samples with 27 wt.% [Emim][OAc] content normally had lower T_g than those with 18 wt.% [Emim][OAc], but a more intense peak height. This could be attributed to the greater plasticisation effect of [Emim][OAc] relative to that of water (Xie et al., 2014). For the samples conditioned at low and medium RH, there was a big difference in how the T_g varied with [Emim][OAc] content (cf. Table 3). For example, for the plasticised G80 samples conditioned at low RH, T_g with 18 wt.% [Emim][OAc] content was 79 °C, which decreased to 57 °C when the [Emim][OAc] content was increased to 27 wt.%. For the RMS samples conditioned at low RH, T_g was 76 °C with 18 wt.% [Emim][OAc] content, while T_g was 61 °C with 27 wt.% [Emim][OAc] content. For both starch samples conditioned at high RH, when the [Emim][OAc] content was 18 wt.%, the peak height was still at a level comparable to those in the cases discussed above; however, when the [Emim][OAc] content was changed to 27 wt.%, a strong and sharp peak representing the glass transition of starch was observed. This apparent transition could be associated with the greater mobility assisted by the highest contents of both [Emim][OAc] and water (resulting from high RH). Nonetheless, for the samples conditioned at high RH (thus with the highest water contents), when the [Emim][OAc] content was changed from 18 wt.% to 27 wt.%, T_g did not vary much, from 52 °C to 49 °C for G80 and from 59 °C to 58 °C for RMS. It is proposed that once the starch macromolecules are saturated with plasticisers, further addition of plasticiser will not change the molecular mobility (reflected by T_g) any further.

[Insert Table 3 here]

3.5. TGA

Our previous report has shown that [Emim][OAc] has an obvious effect in reducing the thermal decomposition temperature of starch-based materials (Xie et al., 2014). The effects of conditioning RH and amylose content were further investigated here and the results are shown in Figure 4. It can be seen that all samples had a major derivative weight percentage peak between 200 °C and 350 °C, after a gentle hump ranging from 50 °C to 170 °C. The large peak can be associated with the breakage of long chains of starch as well as the destruction (oxidation) of the glucose rings (Liu, Yu, Liu, Chen, & Li, 2009b), while the smaller hump can be ascribed to moisture loss from the samples. For the RMS samples, there seemed to be a small shoulder peak between 190 °C and 230 °C, which overlapped with the major peak. This peak can be specifically ascribed to the breakage of starch long chains (Liu et al., 2009b). With a lower amylose/amylopectin ratio (increased molecular weight), this peak moves to a higher temperature, thus merging into the major peak (Liu et al., 2009b). Therefore, for RMS, this small peak could not be seen. Besides this small peak, the results here show no apparent difference in the thermal stability between the samples of different amylose contents as well as those with different water contents (conditioned at different RHs), which is similar to the results for starch with only water (Liu et al., 2009b).

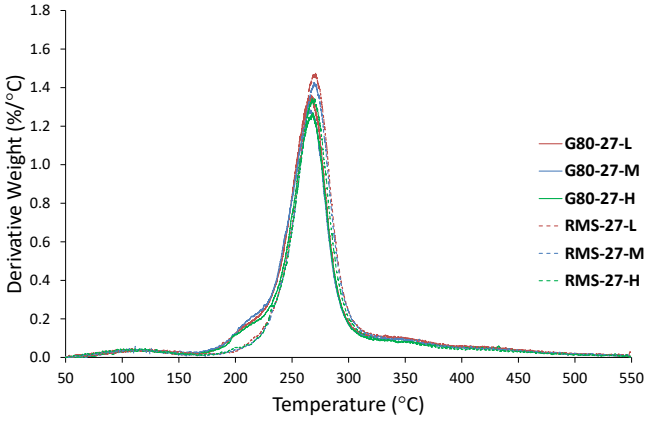

Figure 4 TGA results of the different starch-based films. "L", "M", and "H" (shown by different colours) correspond to samples after conditioning at low (33%), medium (52%) and high (75%) relative humidity.

3.6. Electrical conductivity

The electrical conductivity results for the different samples are shown in Figure 5. It can be seen that the electrical conductivity ranged between $10^{-9.5}$ to $10^{-5.8}$ S/cm for different formulations. Wang et al. (2009a) prepared starch-based films plasticised by 30 wt.% 1-allyl-3-methylimidazolium chloride ([Amim][Cl]), which had electrical conductivity as high as $10^{-1.6}$ S/cm at 14.5 wt.% water content. Sankri et al. (2010) showed that starch-based films plasticised by 30 wt.% 1-butyl-3-methylimidazolium chloride ([Bmim][Cl]) had electrical conductivity of $10^{-4.6}$ S/cm at 13 wt.% water content. Sankri et al. (2010) further proposed that the high electrical conductivity obtained by Wang et al. (2009a) may be explained by increased ion mobility due to the ion pair dissociation mechanism described by Zhang et al. (2005), and this ion pair dissociation might not be apparent for [Amim][Cl] resulting in more localised ions in the case of

[Amim][Cl]–plasticised starch. Also, as the conductivity is mainly controlled by ion diffusivity and mobility, the anion should be small, with delocalized charge. For the lower electrical conductivity of [Emim][OAc]–plasticised starch in this study as compared to those of starch-based materials plasticised by other ILs in the literature, the lower extent of ion pair dissociation and the anion size might be a reason, while the smaller amount (≤ 27%) of IL in starch should also be considered.

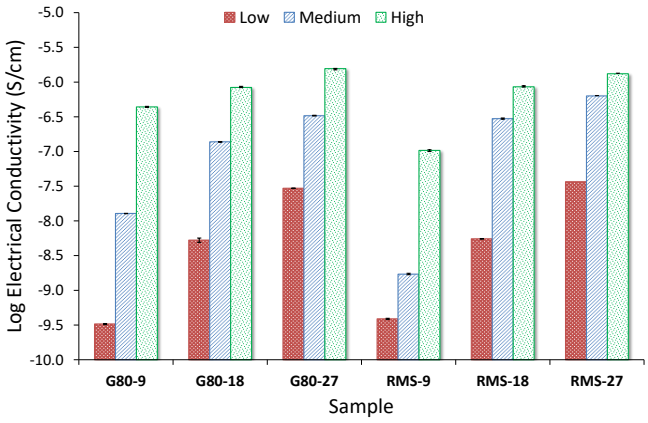

Figure 5 Electrical conductivity of the different starch-based films. The error bars represent standard deviations. "Low", "Medium", and "High" (shown by different colours and patterns) correspond to samples after conditioning at low (33%), medium (52%) and high (75%) relative humidity.

From Figure 5, a general trend could be identified in that both increase in RH and [Emim][OAc] content could increase the electrical conductivity, with the effect of RH being more significant. Wang et al. (2009a) have indicated that increasing ion concentration by increasing the IL content could improve the conductance of plasticised

starch films effectively, and high water content can be advantageous to the transference of the anions and cations in plasticised starch films. Nevertheless, there was no apparent trend regarding the influence of amylose content on electrical conductivity. The plasticised G80 samples with 9% [Emim][OAc] content conditioned at the medium and high RH seemed to have higher electrical conductivity than the plasticised RMS samples with the same [Emim][OAc] content conditioned at the same RHs. But this may need further investigation.

4. Conclusion

It is well established in the literature that the amylose content of starch can greatly influence the structure and properties of starch-based materials. However, this study showed that the amylose content could only have some degree of influence on the crystalline structure and the mobility of the amorphous chain segments in [Emim][OAc]–plasticised starch. Nevertheless, this structural difference was shown to not significantly impact on mechanical properties, glass transition temperature, thermal stability, nor electrical conductivity of plasticised starch films. This may be ascribed in part to the relatively low degree of crystallinity in the starch samples, meaning that the plasticisation of starch macromolecules by [Emim][OAc] and water could play a major role in determining material characteristics. Furthermore, the strong plasticisation effect imparted by [Emim][OAc] compared to other plasticisers could make entanglement of starch macromolecules (mainly amylose) much less significant. As a result, rather than the IL content, RH conditioning and thus the sample water content predominantly

influenced mechanical properties, glass transition temperature, and electrical conductivity.

Overall, this study suggests that, with the strong plasticisation effect of an IL, the effect of amylose content on characteristics of starch-based materials could become unimportant, thus the use of relatively more expensive high-amylose starches can be unnecessary for the formation of mechanically-useful structures in biomaterials applications. This study also shows the potential of IL-plasticised starch-based materials in applications as smart devices where the control of material characteristics by environmental RH is desirable.

Acknowledgements

The research leading to these results has received funding from the Australian Research Council (ARC) under the Discovery Project No. 120100344. M. Li also would like to thank the China Scholarship Council (CSC) for providing research funding for her Ph.D. study at The University of Queensland (UQ). The authors acknowledge the facilities, and the scientific and technical assistance, of the Australian Microscopy & Microanalysis Research Facility (AMMRF) at the Centre for Microscopy and Microanalysis (CMM), UQ.

References

Abe, M., Fukaya, Y., & Ohno, H. (2012). Fast and facile dissolution of cellulose with tetrabutylphosphonium hydroxide containing 40 wt% water. *Chemical Communications, 48*(12), 1808-1810.

Avérous, L. (2004). Biodegradable multiphase systems based on plasticized starch: a review. *Polymer Reviews, 44*(3), 231-274.

Biswas, A., Shogren, R. L., Stevenson, D. G., Willett, J. L., & Bhowmik, P. K. (2006). Ionic liquids as solvents for biopolymers: Acylation of starch and zein protein. *Carbohydrate Polymers, 66*(4), 546-550.

Blazek, J., Salman, H., Rubio, A. L., Gilbert, E., Hanley, T., & Copeland, L. (2009). Structural characterization of wheat starch granules differing in amylose content and functional characteristics. *Carbohydrate Polymers, 75*(4), 705-711.

Chaudhary, A. L., Miler, M., Torley, P. J., Sopade, P. A., & Halley, P. J. (2008). Amylose content and chemical modification effects on the extrusion of thermoplastic starch from maize. *Carbohydrate Polymers, 74*(4), 907-913.

Chaudhary, A. L., Torley, P. J., Halley, P. J., McCaffery, N., & Chaudhary, D. S. (2009). Amylose content and chemical modification effects on thermoplastic starch from maize - Processing and characterisation using conventional polymer equipment. *Carbohydrate Polymers, 78*(4), 917-925.

Cheetham, N. W. H., & Tao, L. (1997). The effects of amylose content on the molecular size of amylose, and on the distribution of amylopectin chain length in maize starches. *Carbohydrate Polymers, 33*(4), 251-261.

Cheetham, N. W. H., & Tao, L. (1998). Variation in crystalline type with amylose content in maize starch granules: an X-ray powder diffraction study. *Carbohydrate Polymers, 36*(4), 277-284.

Chinnaswamy, R., & Hanna, M. A. (1988). Relationship between amylose content and extrusion-expansion properties of corn starches. *Cereal Chemistry, 65*(2), 138-143.

556 Della Valle, G., Colonna, P., Patria, A., & Vergnes, B. (1996). Influence of amylose
557 content on the viscous behavior of low hydrated molten starches. *Journal of*
558 *Rheology, 40*(3), 347-362.
559 El Seoud, O. A., Koschella, A., Fidale, L. C., Dorn, S., & Heinze, T. (2007). Applications
560 of ionic liquids in carbohydrate chemistry: A window of opportunities.
561 *Biomacromolecules, 8*(9), 2629-2647.
562 Forssell, P., Lahtinen, R., Lahelin, M., & Myllärinen, P. (2002). Oxygen permeability of
563 amylose and amylopectin films. *Carbohydrate Polymers, 47*(2), 125-129.
564 Fu, Z.-q., Wang, L.-j., Li, D., Wei, Q., & Adhikari, B. (2011). Effects of high-pressure
565 homogenization on the properties of starch-plasticizer dispersions and their films.
566 *Carbohydrate Polymers, 86*(1), 202-207.
567 Fukaya, Y., Sugimoto, A., & Ohno, H. (2006). Superior solubility of polysaccharides in
568 low viscosity, polar, and halogen-free 1, 3-dialkylimidazolium formates.
569 *Biomacromolecules, 7*(12), 3295-3297.
570 Hall, C. A., Le, K. A., Rudaz, C., Radhi, A., Lovell, C. S., Damion, R. A., et al. (2012).
571 Macroscopic and microscopic study of 1-ethyl-3-methyl-imidazolium acetate–water
572 mixtures. *The Journal of Physical Chemistry B, 116*(42), 12810-12818.
573 Heinze, T., Schwikal, K., & Barthel, S. (2005). Ionic liquids as reaction medium in
574 cellulose functionalization. *Macromolecular Bioscience, 5*(6), 520-525.
575 Jane, J.-l. (2009). Structural features of starch granules II. In B. James, & W. Roy (Eds.),
576 *Starch (Third Edition)* (pp. 193-236). San Diego: Academic Press.
577 Jenkins, P. J., & Donald, A. M. (1995). The influence of amylose on starch granule
578 structure. *International Journal of Biological Macromolecules, 17*(6), 315-321.

579 Leroy, E., Jacquet, P., Coativy, G., Reguerre, A. l., & Lourdin, D. (2012).
580 Compatibilization of starch–zein melt processed blends by an ionic liquid used as
581 plasticizer. *Carbohydrate Polymers, 89*(3), 955-963.
582 Li, M., Liu, P., Zou, W., Yu, L., Xie, F., Pu, H., et al. (2011). Extrusion processing and
583 characterization of edible starch films with different amylose contents. *Journal of*
584 *Food Engineering, 106*(1), 95-101.
585 Liew, C.-W., Ramesh, S., Ramesh, K., & Arof, A. (2012). Preparation and
586 characterization of lithium ion conducting ionic liquid-based biodegradable corn
587 starch polymer electrolytes. *Journal of Solid State Electrochemistry, 16*(5), 1869-
588 1875.
589 Liu, H., Yu, L., Xie, F., & Chen, L. (2006). Gelatinization of cornstarch with different
590 amylose/amylopectin content. *Carbohydrate Polymers, 65*(3), 357-363.
591 Liu, H., Xie, F., Yu, L., Chen, L., & Li, L. (2009a). Thermal processing of starch-based
592 polymers. *Progress in Polymer Science, 34*(12), 1348-1368.
593 Liu, P., Xie, F., Li, M., Liu, X., Yu, L., Halley, P. J., et al. (2011). Phase transitions of
594 maize starches with different amylose contents in glycerol-water systems.
595 *Carbohydrate Polymers*, *85*(1), 180-187.
596 Liu, W.-C., Halley, P. J., & Gilbert, R. G. (2010). Mechanism of degradation of starch, a
597 highly branched polymer, during extrusion. *Macromolecules, 43*(6), 2855-2864.
598 Liu, X., Yu, L., Liu, H., Chen, L., & Li, L. (2009b). Thermal decomposition of corn
599 starch with different amylose/amylopectin ratios in open and sealed systems. *Cereal*
600 *Chemistry, 86*(4), 383-385.

Lopez-Rubio, A., Flanagan, B. M., Gilbert, E. P., & Gidley, M. J. (2008). A novel approach for calculating starch crystallinity and its correlation with double helix content: A combined XRD and NMR study. *Biopolymers, 89*(9), 761-768.

Lourdin, D., Della Valle, G., & Colonna, P. (1995). Influence of amylose content on starch films and foams. *Carbohydrate Polymers, 27*(4), 261-270.

Lu, J., Yan, F., & Texter, J. (2009). Advanced applications of ionic liquids in polymer science. *Progress in Polymer Science, 34*(5), 431-448.

Madrigal, L., Sandoval, A. J., & Müller, A. J. (2011). Effects of corn oil on glass transition temperatures of cassava starch. *Carbohydrate Polymers, 85*(4), 875-884.

Mateyawa, S., Xie, D. F., Truss, R. W., Halley, P. J., Nicholson, T. M., Shamshina, J. L., et al. (2013). Effect of the ionic liquid 1-ethyl-3-methylimidazolium acetate on the phase transition of starch: Dissolution or gelatinization? *Carbohydrate Polymers, 94*(1), 520-530.

Mondragón, M., Mancilla, J. E., & Rodríguez-González, F. J. (2008). Nanocomposites from plasticized high-amylopectin, normal and high-amylose maize starches. *Polymer Engineering & Science, 48*(7), 1261-1267.

Perdomo, J., Cova, A., Sandoval, A. J., García, L., Laredo, E., & Müller, A. J. (2009). Glass transition temperatures and water sorption isotherms of cassava starch. *Carbohydrate Polymers, 76*(2), 305-313.

Pérez, S., Baldwin, P. M., & Gallant, D. J. (2009). Structural features of starch granules I. In B. James, & W. Roy (Eds.), *Starch (Third Edition)* (pp. 149-192). San Diego: Academic Press.

623 Pérez, S., & Bertoft, E. (2010). The molecular structures of starch components and their
624 contribution to the architecture of starch granules: a comprehensive review.
625 *Starch/Stärke*, *62*(8), 389-420.
626 Phillips, D. M., Drummy, L. F., Conrady, D. G., Fox, D. M., Naik, R. R., Stone, M. O., et
627 al. (2004). Dissolution and regeneration of bombyx mori silk fibroin using ionic
628 liquids. *Journal of the American Chemical Society*, *126*(44), 14350-14351.
629 Pu, Y., Jiang, N., & Ragauskas, A. J. (2007). Ionic Liquid as a Green Solvent for Lignin.
630 *Journal of Wood Chemistry and Technology*, *27*(1), 23-33.
631 Ramesh, S., Liew, C.-W., & Arof, A. K. (2011). Ion conducting corn starch biopolymer
632 electrolytes doped with ionic liquid 1-butyl-3-methylimidazolium
633 hexafluorophosphate. *Journal of Non-Crystalline Solids*, *357*(21), 3654-3660.
634 Ramesh, S., Shanti, R., Morris, E., & Durairaj, R. (2011). Utilisation of corn starch in
635 production of 'green' polymer electrolytes. *Materials Research Innovations*, *15*(1), s8.
636 Ramesh, S., Shanti, R., & Morris, E. (2012). Studies on the thermal behavior of
637 CS:LiTFSI:[Amim] Cl polymer electrolytes exerted by different [Amim] Cl content.
638 *Solid State Sciences*, *14*(1), 182-186.
639 Remsing, R. C., Swatloski, R. P., Rogers, R. D., & Moyna, G. (2006). Mechanism of
640 cellulose dissolution in the ionic liquid 1-n-butyl-3-methylimidazolium chloride: a 13
641 C and 35/37 Cl NMR relaxation study on model systems. *Chemical*
642 *Communications*(12), 1271-1273.
643 Rindlav-Westling, A., Stading, M., & Gatenholm, P. (2001). Crystallinity and
644 morphology in films of starch, amylose and amylopectin blends. *Biomacromolecules*,
645 *3*(1), 84-91.

Rindlav-Westling, Å., Stading, M., Hermansson, A.-M., & Gatenholm, P. (1998). Structure, mechanical and barrier properties of amylose and amylopectin films. *Carbohydrate Polymers, 36*(2–3), 217-224.

Sankri, A., Arhaliass, A., Dez, I., Gaumont, A. C., Grohens, Y., Lourdin, D., et al. (2010). Thermoplastic starch plasticized by an ionic liquid. *Carbohydrate Polymers, 82*(2), 256-263.

Shi, Y.-C., Capitani, T., Trzasko, P., & Jeffcoat, R. (1998). Molecular structure of a low-amylopectin starch and other high-amylose maize starches. *Journal of Cereal Science, 27*(3), 289-299.

Tan, I., Flanagan, B. M., Halley, P. J., Whittaker, A. K., & Gidley, M. J. (2007). A method for estimating the nature and relative proportions of amorphous, single, and double-helical components in starch granules by ^{13}C CP/MAS NMR. *Biomacromolecules, 8*(3), 885-891.

van Soest, J. J. G., Hulleman, S. H. D., de Wit, D., & Vliegenthart, J. F. G. (1996). Crystallinity in starch bioplastics. *Industrial Crops and Products, 5*(1), 11-22.

van Soest, J. J. G., & Borger, D. B. (1997). Structure and properties of compression-molded thermoplastic starch materials from normal and high-amylose maize starches. *Journal of Applied Polymer Science, 64*(4), 631-644.

Wang, J., Yu, L., Xie, F., Chen, L., Li, X., & Liu, H. (2010a). Rheological properties and phase transition of cornstarches with different amylose/amylopectin ratios under shear stress. *Starch/Stärke, 62*(12), 667-675.

667 Wang, N., Zhang, X., Liu, H., & He, B. (2009a). 1-Allyl-3-methylimidazolium chloride
668 plasticized-corn starch as solid biopolymer electrolytes. *Carbohydrate Polymers,*
669 *76*(3), 482-484.
670 Wang, N., Zhang, X., Wang, X., & Liu, H. (2009b). Communications: Ionic liquids
671 modified montmorillonite/thermoplastic starch nanocomposites as ionic conducting
672 biopolymer. *Macromolecular Research, 17*(5), 285-288.
673 Wang, N., Zhang, X., Liu, H., & Han, N. (2010b). Ionically conducting polymers based
674 on ionic liquid-plasticized starch containing lithium chloride. *Polymers & Polymer*
675 *Composites, 18*(1), 53-58.
676 Wang, Q., Chen, Q., Yang, Y., & Shao, Z. (2012). Effect of various dissolution systems
677 on the molecular weight of regenerated silk fibroin. *Biomacromolecules, 14*(1), 285-
678 289.
679 Wang, Q., Yang, Y., Chen, X., & Shao, Z. (2012). Investigation of rheological properties
680 and conformation of silk fibroin in the solution of AmimCl. *Biomacromolecules,*
681 *13*(6), 1875-1881.
682 Wilpiszewska, K., & Spychaj, T. (2011). Ionic liquids: Media for starch dissolution,
683 plasticization and modification. *Carbohydrate Polymers, 86*(2), 424-428.
684 Wu, Y., Sasaki, T., Irie, S., & Sakurai, K. (2008). A novel biomass-ionic liquid platform
685 for the utilization of native chitin. *Polymer, 49*(9), 2321-2327.
686 Xie, F., Yu, L., Su, B., Liu, P., Wang, J., Liu, H., et al. (2009). Rheological properties of
687 starches with different amylose/amylopectin ratios. *Journal of Cereal Science, 49*(3),
688 371-377.

689 Xie, F., Halley, P. J., & Avérous, L. (2012). Rheology to understand and optimize
690 processibility, structures and properties of starch polymeric materials. *Progress in*
691 *Polymer Science, 37*(4), 595-623.
692 Xie, F., Pollet, E., Halley, P. J., & Avérous, L. (2013). Starch-based nano-biocomposites.
693 *Progress in Polymer Science, 38*(10-11), 1590-1628.
694 Xie, F., Flanagan, B. M., Li, M., Sangwan, P., Truss, R. W., Halley, P. J., et al. (2014).
695 Characteristics of starch-based films plasticised by glycerol and by the ionic liquid 1-
696 ethyl-3-methylimidazolium acetate: a comparative study. *Carbohydrate Polymers,*
697 *111*, 841-848.
698 Xie, H., Li, S., & Zhang, S. (2005). Ionic liquids as novel solvents for the dissolution and
699 blending of wool keratin fibers. *Green Chemistry, 7*(8), 606-608.
700 Xie, H., Zhang, S., & Li, S. (2006). Chitin and chitosan dissolved in ionic liquids as
701 reversible sorbents of CO_2. *Green Chemistry, 8*(7), 630-633.
702 Yu, L., Dean, K., & Li, L. (2006). Polymer blends and composites from renewable
703 resources. *Progress in Polymer Science, 31*(6), 576-602.
704 Zakrzewska, M. E., Bogel-Łukasik, E., & Bogel-Łukasik, R. (2010). Solubility of
705 carbohydrates in ionic liquids. *Energy & Fuels, 24*(2), 737-745.
706 Zhang, C., Liu, R., Xiang, J., Kang, H., Liu, Z., & Huang, Y. (2014). Dissolution
707 Mechanism of Cellulose in N, N-Dimethylacetamide/Lithium Chloride: Revisiting
708 through Molecular Interactions. *The Journal of Physical Chemistry B*.
709 Zhang, H., Wu, J., Zhang, J., & He, J. (2005). 1-Allyl-3-methylimidazolium chloride
710 room temperature ionic liquid: A new and powerful nonderivatizing solvent for
711 cellulose. *Macromolecules, 38*(20), 8272-8277.

712 Zhu, S., Wu, Y., Chen, Q., Yu, Z., Wang, C., Jin, S., et al. (2006). Dissolution of
713 cellulose with ionic liquids and its application: a mini-review. *Green Chemistry, 8*(4),
714 325-327.
715

Figure captions

Figure 1 XRD results of G80 and RMS native starches and the different starch-based films. "L", "M", and "H" (shown by different colours) correspond to samples after conditioning at low (33%), medium (52%) and high (75%) relative humidity.

Figure 2 Tensile strength (σ_t) (upper), Young's modulus (E) (middle), and elongation at break (ε_b) (lower) of the different starch-based films. The error bars represent standard deviations. "Low", "Medium", and "High" (shown by different colours and patterns) correspond to samples after conditioning at low (33%), medium (52%) and high (75%) relative humidity.

Figure 3 tan δ of the different starch-based films (top: G80; bottom: RMS). "L", "M", and "H" (shown by different colours) correspond to samples after conditioning at low (33%), medium (52%) and high (75%) relative humidity.

Figure 4 TGA results of the different starch-based films. "L", "M", and "H" (shown by different colours) correspond to samples after conditioning at low (33%), medium (52%) and high (75%) relative humidity.

Figure 5 Electrical conductivity of the different starch-based films. The error bars represent standard deviations. "Low", "Medium", and "High" (shown by different colours and patterns) correspond to samples after conditioning at low (33%), medium (52%) and high (75%) relative humidity.

737 **Tables**

738 Table 1 Samples codes, formulations, and relative humidity during conditioning, of the starch-based films.

Code	Formulation[a]					Conditioning
	Starch type	Starch content[b]	[Emim][OAc] content	Water content (original)[c]	Water content (post-conditioning)	Relative humidity (%)
G80-9-L	Gelose 80	85.9	9	35.1	7.60±0.29[d]	33
G80-9-M		85.9	9	35.1	11.35±0.18	52
G80-9-H		85.9	9	35.1	14.22±0.20	75
G80-18-L		85.9	18	26.1	7.36±0.18	33
G80-18-M		85.9	18	26.1	12.88±0.12	52
G80-18-H		85.9	18	26.1	20.12±0.16	75
G80-27-L		85.9	27	17.1	8.94±0.08	33
G80-27-M		85.9	27	17.1	17.16±0.14	52
G80-27-H		85.9	27	17.1	27.94±0.24	75
RMS-9-L	Regular maize starch	85.6	9	35.4	8.34±0.05	33
RMS-9-M		85.6	9	35.4	11.78±0.27	52

RMS-9-H	85.6	9	35.4	14.87±0.25	75
RMS-18-L	85.6	18	26.4	8.00±0.11	33
RMS-18-M	85.6	18	26.4	12.35±0.11	52
RMS-18-H	85.6	18	26.4	20.69±0.08	75
RMS-27-L	85.6	27	17.4	9.04±0.08	33
RMS-27-M	85.6	27	17.4	15.96±0.22	52
RMS-27-H	85.6	27	17.4	27.84±0.06	75

739 [a] Portions in weight; [b] Dry weight; [c] Combination of added water and original moisture content in starch; [d] Standard deviation

740

741 Table 2 XRD and ^{13}C CP/MAS NMR results of the starch-based films

Sample	XRD Results			^{13}C CP/MAS NMR Results			
	Double helix	V-type	Amorphous	Double helix	V-type	Rigid amorphous	Mobile amorphous
Native G80	32.2	ND[a]	–	–	–	–	–
G80-18-L	22.4	8.4	69.2	20.0	10.8	41.6	27.6
G80-18-M	18.4	9.4	72.2	17.5	10.3	46.3	25.9
G80-18-H	21.2	8.2	70.5	20.4	9.1	48.6	21.9
Native RMS	39.5	ND[a]	–	–	–	–	–
RMS-18-L	19.7	4.8	75.5	17.7	6.8	60	15.5
RMS-18-M	18	4.8	77.2	15.9	6.9	57.1	20.1
RMS-18-H	18.4	5.1	76.5	17.5	6.0	57.9	18.6

742 [a] Unable to be determined as the V-type crystallinity pattern was difficult to be differentiated from the A or B-type crystallinity pattern

743

744 Table 3 Glass transition temperatures (T_g) of the starch-based films

Sample	T_g (°C)
G80-18-L	79
G80-18-M	63
G80-18-H	52
G80-27-L	57
G80-27-M	52
G80-27-H	49
RMS-18-L	76
RMS-18-M	73
RMS-18-H	59
RMS-27-L	61
RMS-27-M	56
RMS-27-H	58

745